

# Study of the Borromean dripline nucleus $^{17}\text{Ne}$

F. Aksouh, Yu. Aksyutina, T. Aumann, K. Boretzky, T. Le Blais, M.J.G. Borge, L.V. Chulkov, D. Cortina-Gil, J.E. Ducret, H. Emling, J. Enders, C. Forssén, L.M. Fraile, H.O.U. Fynbo, H. Geissel, L.V. Grigorenko, H. Jeppesen, H.T. Johansson, B. Jonson, R. Kanungo, O. Kiselev, J.V. Kratz, R. Kulesa, H. Lenske, A. Lindahl, M. Meister, T. Nilsson, G. Nyman, Yu.L. Parfenova, A. Richter, K. Riisager, G. Schrieder, N.B. Shulgina, H. Simon, K. Sümmerer, O. Tengblad, H. Weick, and M.V. Zhukov

## Abstract

This proposal aims at a study of  $^{17}\text{Ne}$  at the ALADIN-LAND/R<sup>3</sup>B setup in Cave C.  $^{17}\text{Ne}$  is a Borromean dripline nucleus (the binary subsystems  $p-p$  and  $^{15}\text{O}-p$  are unbound) and the only realistic candidate to show a two-proton halo in its ground state.

## Proposal

We have conducted an experimental programme to study halo-states in nuclei at GSI since 1992. The experiments have been performed both with the FRS and with the ALADIN-LAND setup in Cave B. The early results were mainly on carbon and lead targets. In the most recent experiment in our series we have used a liquid H<sub>2</sub> target. The analysis of the data from this experiment, **S245**, is well underway and the first results with beams of  $^8\text{He}$ ,  $^{11}\text{Li}$  and  $^{14}\text{Be}$  are emerging. The remaining beamtime for **S245** is planned for the spring of 2006, where  $^{19}\text{C}$  and  $^{22,23}\text{N}$  will be studied in our modified setup with MINIBALL clusters at the FRS.

Here we propose a continuation of our programme concentrating on one single nucleus,  $^{17}\text{Ne}$ . This proton dripline nucleus has a half-life of  $T_{1/2} = 109.2$  ms, and can be obtained as a radioactive beam from the SIS using a primary  $^{20}\text{Ne}$  beam with an energy of 500 MeV/u. The primary beam hits a Be production target placed at the entrance of the FRS and the separated secondary  $^{17}\text{Ne}$  beam is then brought to the reaction target in the LAND/R<sup>3</sup>B setup in Cave C.

Our experiments will be organized as follows:

- (1) Nuclear break up will be studied with targets CH<sub>2</sub> and carbon.
- (2) Coulomb breakup will be studied using a lead target.

## Present knowledge about $^{17}\text{Ne}$

$^{17}\text{Ne}$  is the lightest bound isotope of neon. Its two proton separation energy is  $S_{2p} = 950$  keV and its binary subsystems,  $p-p$  and  $^{16}\text{F}$ , are unbound. This Borromean character of  $^{17}\text{Ne}$  combined with its low two-proton separation energy makes it an obvious candidate to be a two-proton halo nucleus [1, 2].

The  $\beta$  delayed proton and  $\alpha$  emission from  $^{17}\text{Ne}$  has been studied extensively [3] and the feeding to excited states in its daughter nucleus  $^{17}\text{F}$  has been measured. The first-forbidden beta-decay to the first excited state in  $^{17}\text{F}$  at 495 keV was studied [4–6] in order to try to investigate a possible signal of a halo character by a comparison to the mirror decay of  $^{17}\text{N}$  into the 871 keV state in  $^{17}\text{O}$  [7]. The branching ratio of 1.59(17)% is about two times larger than

expected from mirror symmetry. This very large asymmetry was explained in a shell-model calculation [4] as being due to the unusually large spatial extent of the  $1s_{1/2}$  proton orbit. It has also been suggested that an alternative explanation to the asymmetry would lie in a charge-dependent  $s$ -occupancy for the initial state [8].

The rms radii for the  $A=17$  isobars were extracted from measurements of interaction cross sections at an energy of  $\sim 700$  MeV/u [9] and the results for the mirror pair  $^{17}\text{Ne} - ^{17}\text{N}$  were  $R_{rms}^m = 2.75(07)$  and  $2.48(05)$ , respectively. This difference in the radii was considered as being due to an anomalous structure of  $^{17}\text{Ne}$ . An increase in the total reaction cross section for  $^{17}\text{Ne}$  relative to its neighbour was also observed in measurements with a Si target at 40 MeV/u [10]. Tanaka et al. [11] measured  $\sigma_R$  with the transmission method and used these and the high energy data [9] to derive the density distribution from a Glauber calculation in the optical limit. The result showed a long tail in the density distribution, which they interpreted as evidence for the two valence protons being in the  $1s_{1/2}$  orbital.

With a 66 MeV/u  $^{17}\text{Ne}$  beam from the RIPS separator at RIKEN, Kanungo et al. [12] measured the two-proton removal cross section and the  $^{15}\text{O}$  momentum distribution. The narrow momentum width of 168(17) MeV/c together with the large proton removal cross section (191(48) mb) were taken as indication of a significant  $s$ -wave probability of the two valence protons and an evidence of  $^{17}\text{Ne}$  being a two-proton halo nucleus. Further evidence for a halo structure in  $^{17}\text{Ne}$  is given by the measured momentum width after two-proton removal from  $^{15}\text{O}$  [13]. This is found to be much wider than that for  $^{17}\text{Ne}$  and in close agreement with the Goldhaber estimate. This suggests that the two valence protons in  $^{17}\text{Ne}$  have a significant probability to form a halo around the  $^{15}\text{O}$  core.

Experiments on Coulomb excitation of the two lowest, two-proton unstable excited states in  $^{17}\text{Ne}$  at 344 keV ( $3/2^-$ ) and 906 keV ( $5/2^-$ ) above the  $^{15}\text{O}+p+p$  threshold, respectively, have been performed [14,15]. Both these states are unbound to two-proton emission but the  $I^\pi=3/2^-$  state is too low in energy to allow two-proton emission while the  $I^\pi=5/2^-$  state has been observed to decay via sequential two-proton emission to the  $^{15}\text{O}$  ground state.

Even though there obviously exists a fair amount of data on  $^{17}\text{Ne}$  and its decay there are no clear conclusions about the structure of  $^{17}\text{Ne}$  that might be drawn from the present results. One important issue is the relative contribution of  $s^2$  and  $d^2$  configuration in the  $^{17}\text{Ne}$  wave function. There exist rather detailed structural calculations that include spin degrees of freedom properly [17,18], theoretical estimates of the  $s/d$  ratio [16] and theoretical suggestions for important experimental observables [19]. The time is thus ripe to do a state-of-the-art study of  $^{17}\text{Ne}$  with our complete-kinematics setup in Cave C.

The continuum states in  $^{17}\text{Ne}$  are also of interest for nuclear astrophysics. The  $rp$  reaction flow for nucleosynthesis in explosive hydrogen burning in stars is influenced by two-proton reactions on long-lived waiting point nuclei as discussed in Ref. [23]. The rate estimates in this paper were obtained in a model where the reactions were characterized by two successive proton captures; the first capture leads to an unbound isotope and the system is then stabilized by a second proton capture. One such reaction discussed in [23] is  $^{15}\text{O}(2p,\gamma)^{17}\text{Ne}$ . Recent calculations [24,25] have, however, demonstrated that the continuum states ( $^{15}\text{O} + 2p$ ) plays an important role for the calculated rate. It is found [24,25] that the rate can be enhanced by 10 orders of magnitude by taking an exact account of the three-body continuum in for example  $^{17}\text{Ne}$ .

With this starting point we would here propose a complete kinematics experiment to be performed at GSI. Our main objectives are summarized in the next section.

## Proposed experiments

Our intention is to perform a “kinematically complete” experiment with detection of the charged projectile fragments in the exit channel together with coincident gamma rays from the projectile and the fragments. With a primary  $^{20}\text{Ne}$  beam from the SIS a secondary  $^{17}\text{Ne}$  beam of 500 MeV/u will be produced using a Be production target. The reaction target will be placed at the entrance of the ALADIN magnet and we propose to use three different targets to collect the maximum of information. For details see next Section.

Below we give the main data sets that we will be able to collect

- *Nuclear interaction and proton removal cross sections.*

We propose to perform measurements of nuclear interaction and proton removal cross sections using light reaction targets. We may study the following three different reaction channels:

- Detection of two protons in coincidence with the charged fragment ( $^{15}\text{O}$ ) corresponds to a quasi-sequential process – excitation of  $^{17}\text{Ne}$  as a single system to the continuum followed by its decay. The reaction mechanism might be either diffractive dissociation or inelastic scattering. This reaction mechanism allows to study the structure of the  $^{17}\text{Ne}$  continuum and to separate resonance states. These types of reactions are referred to as the *inelastic scattering channel* with cross section  $\sigma_{2p}$ .

- Detection of only one proton means that the second one has either been absorbed or has got a large momentum transfer and been deflected strongly. Such a reaction corresponds to the one-proton knock-out mechanism. This channel is referred to as the *proton knock-out channel*,  $\sigma_{1p}$ .

- Reactions where only the charged fragment in the vicinity of the fragmentation peak is detected is referred to as the *two-proton knock-out channel*,  $\sigma_{0p}$ .

These cross sections may be calculated in the eikonal approximation of the Glauber model in a three-body treatment of  $^{17}\text{Ne}$ . The well-known relation between the breakup and interaction cross sections are then

$$\sigma_I(^{17}\text{Ne}) - \sigma_I(^{15}\text{O}) = \sigma_{-2p} = \sigma_{0p} + \sigma_{1p} + \sigma_{2p}, \quad (1)$$

The one-proton knockout reactions from  $^{17}\text{Ne}$  is expected to be due partly to proton removal from the halo leading to low lying negative parity states in  $^{16}\text{F}$  [19]. The  $s_{1/2} \otimes ^{15}\text{O}(1/2^-)$  and  $d_{5/2} \otimes ^{15}\text{O}(1/2^-)$  components result in  $I^\pi=0^-, 1^-, 2^-, 3^-$   $^{16}\text{F}$  states exhausting about 2/3 of the cross section [19], while the rest may be due to proton knockout from the core leading to highly excited positive parity states in  $^{16}\text{F}$  with  $I^\pi=1^+$  ( $^{14}\text{N}(1^+) \otimes (s_{1/2})^2(0^+)$ ) The complete kinematics data allows the construction of the  $^{16}\text{F}$  invariant mass spectrum for both these reaction channels and can be used to separate them from each other.

The expected magnitude of the nuclear induced breakup cross section has been estimated with the eikonal approximation of the Glauber model. The main ingredients in the eikonal approximation are the three-body wavefunction for  $^{17}\text{Ne}$  ( $^{15}\text{O}+p+p$ ) and profile functions of the cluster-target interaction.

The estimated  $^{17}\text{Ne}$  interaction cross section on a C target at an energy of 500 MeV/u varies from 969 mb ( $\text{rms}(^{15}\text{O})=2.40$  fm) to 994 mb ( $\text{rms}(^{15}\text{O})=2.52$  fm).

In the case of the spectator  $^{15}\text{O}$ , the two-proton removal cross section  $\sigma_{-2p}$  is found as the difference between the  $^{17}\text{Ne}$  and  $^{15}\text{O}$  interaction cross sections,  $\sigma_{-2p} = \sigma_I(^{17}\text{Ne}) - \sigma_I(^{15}\text{O})$  ( $\sim 70\text{-}75$  mb). As shown in [19], this cross section should be corrected for a contribution by proton removal from the  $^{15}\text{O}$  core. This contribution is estimated in the core+proton model of  $^{15}\text{O}$  (see [19]), taking into account excited states of the  $^{14}\text{N}$  core.

The one-proton removal cross section from the  $^{15}\text{O}$  core varies from 47.0 mb to 43.5 mb, respectively. As the result, the total cross section of the two-proton removal from  $^{17}\text{Ne}$  leading to  $^{15}\text{O}$  core production, is estimated as  $\sim 108 - 114$  mb.

- *Transverse momentum distribution*

In experiments on three-body halo systems, reactions in which the core and one of the valence particles are detected are referred to as one-particle knockout (or stripping) reactions. In the sudden approximation, the momentum transfer to the (A-1) system can be neglected in experiments with high beam energy. In the  $^{17}\text{Ne}$  rest frame we have  $\mathbf{p}_{p_1} + \mathbf{p}_{p_2} + \mathbf{p}_{^{15}\text{O}} = 0$ . The momentum of the (A-1) system is then equal to the momentum of the ejected proton  $\mathbf{p}_{n_1}$  with opposite sign and will therefore directly reflect the internal proton momentum distribution.

This ‘‘classical’’ search for a halo signal is well motivated since it gives a rather simple handle on the *s/d* configuration mixing in the  $^{17}\text{Ne}$  ground state. In the recent theoretical paper by Grigorenko et al. [19] it is stated that an *s* wave component exceeding 50 % would give a momentum width of size comparable to  $^6\text{He}$  - a classical halo case. However, as also pointed out, the somewhat larger width found experimentally at 66 MeV/u [12] could be understood by a careful treatment of the reaction mechanism.

- *Angular distribution of the decay proton from the unbound  $^{16}\text{F}$  system*

The angular distribution of the decay neutron from different unbound subsystems of Borromean nuclei have been studied in our earlier experiments at GSI. Figure 1 shows these kind of data. The angular correlation data may be used to get information about configuration mixing in the ground state as was demonstrated for  $^6\text{He}$  [27] in Ref. [28] and for  $^{11}\text{Li}$  where a mixed parity in the ground state was seen in a model-independent way by the presence of a linear term in the angular correlation function [30]. Similar data for the decaying  $^{16}\text{F}$  system will become available in the experiment proposed here.

- *Relative energy distribution in the  $^{15}\text{O-p}$  system*

From the data from this proposal we will be able to reconstruct and study the relative energy spectra between the proton and  $^{15}\text{O}$  in the unbound  $^{16}\text{F}$  system. Such data will provide an opportunity to separate the process of one-proton removal from the  $^{17}\text{Ne}$  proton halo, leading to low relative energies, from the corresponding one-proton removal process from the  $^{15}\text{O}$  core leading to highly excited  $1^+$  states in the unbound  $^{16}\text{F}$ .

- *Continuum excitations in  $^{17}\text{Ne}$*

We may study continuum excitations in  $^{17}\text{Ne}$  by analysis of the two protons and the  $^{15}\text{O}$  core in the final state after the breakup reactions in the carbon and lead targets.

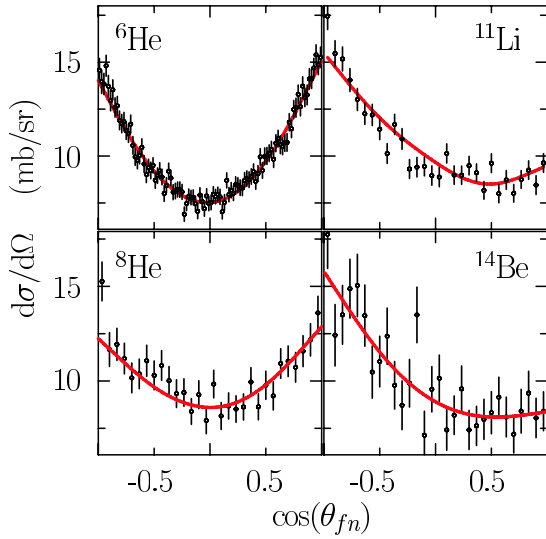


Figure 1: Differential cross section as function of the angle  $\theta_{fn}$  between the momentum of the recoiling  $A - 1$  system (sum of fragment ( $f$ ) and neutron ( $n$ ) momenta) and the relative momentum between fragment and neutron (difference of their momenta). Data are shown for the breakup products of  ${}^6,8\text{He}$  [27, 29],  ${}^{11}\text{Li}$  [30], and  ${}^{14}\text{Be}$ . The solid lines represent polynomial fits in  $\cos(\theta_{fn})$  to the data, including corrections for experimental effects.

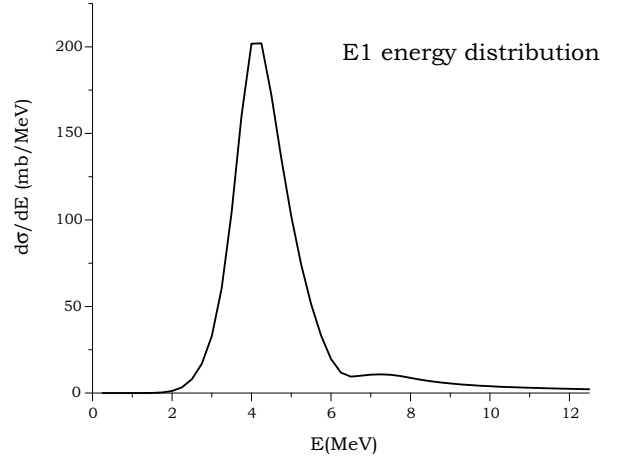


Figure 2: Calculated E1 energy distribution under the assumption of 50 %  $s^2$  and 50 %  $d^2$  components in the  ${}^{17}\text{Ne}$  ground state wave function.

With the carbon target we may study the excited states in  ${}^{17}\text{Ne}$ , which would add to the present knowledge of excited states in  ${}^{17}\text{Ne}$  that until now was obtained mainly in multi-neutron transfer reactions  ${}^{20}\text{Ne}({}^3\text{He}, {}^6\text{He}){}^{17}\text{Ne}$  [31]. The excitation cross-section may be compared to theory in a Glauber model calculation and be used in the analysis of the data from the Pb target to disentangle the relative nuclear and Coulomb contributions to the cross section.

The estimated energy distribution [25] for  $E1$  Coulomb dissociation of  ${}^{17}\text{Ne}$  is shown in Fig. 2. This calculation suggests a pronounced peak at about 4.5 MeV excitation energy with a width of about 2 MeV. The cross section at maximum depends strongly on the  $s$ -wave content in the  ${}^{17}\text{Ne}$  ground-state wave function and becomes higher for an increasing  $s^2$  component.

- *Angular and energy correlations*

With complete kinematics data one may study the dissociation of  ${}^{17}\text{Ne}$  on a lead target and determine the four-momenta of the protons in coincidence with  ${}^{15}\text{O}$ . These are then used to reconstruct the three-body energy and angular correlations in the final state. Such data have recently been analyzed for  ${}^6\text{He}$  [26] and it was shown that important information may be obtained with this approach. With a series expansion of the final

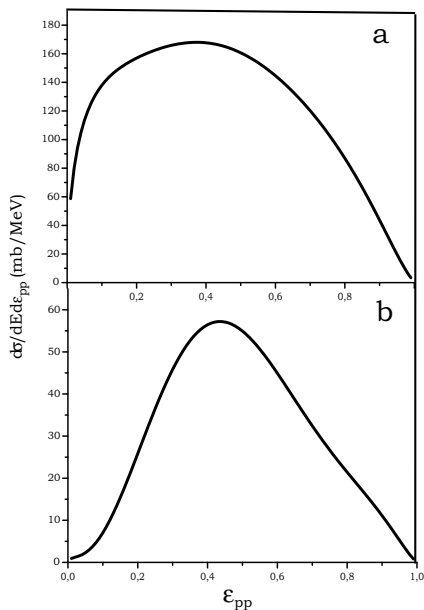


Figure 3: Relative  $\epsilon_{pp}$  distribution of Coulomb breakup of  $^{17}\text{Ne}$  calculated in a three-body  $^{15}\text{O}+p+p$  model [25]. The upper  $\epsilon_{pp}$  distribution (a) is calculated under the assumption of equal  $s^2$  and  $d^2$  occupancy while the distribution (b) is for a pure  $d^2$  configuration. ( $E_{beam}=500$  MeV/u,  $b_{min} = 9.7$  fm,  $E=4.5$  MeV.)

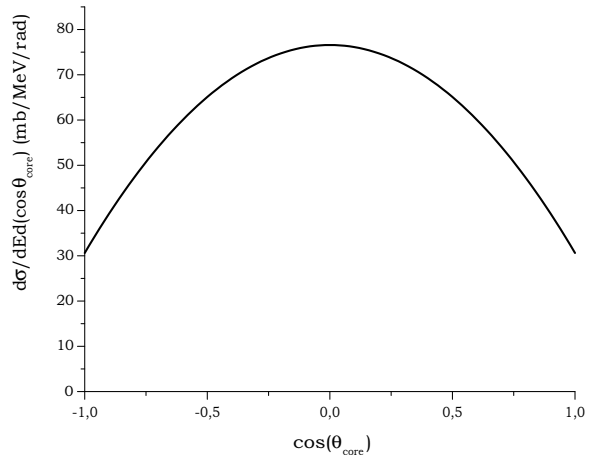


Figure 4: Calculated angular distribution of the  $^{15}\text{O}$  core relative to the beam direction after Coulomb breakup of  $^{17}\text{Ne}$ . ( $E_{beam}=500$  MeV/u,  $b_{min} = 9.7$  fm,  $E=4.5$  MeV.)

transition amplitude into hyperspherical harmonics it was shown that the information of all the three particles in the final state is essential for a theoretical understanding of the structure. The three-body angular and fractional energy correlations may give important information about final-state interactions and about intermediate resonances in the dissociation process.

Figure 3 shows a calculation of the relative energy distribution in the  $pp$ -system at  $E=4.5$  MeV where Figure 3a represents the result with a wave function from Ref. [19] with equal  $s^2$  and  $d^2$  components while Figure 3b show the result under the assumption of a pure  $d^2$  configuration. The clear difference in the shapes demonstrates that we might get a safe determination of the  $s$  -  $d$  mixing from the data.

The calculated angular distribution [25] of the  $^{15}\text{O}$  core after Coulomb dissociation of  $^{17}\text{Ne}$  is shown in Figure 4. The shape of the distribution might be described by a function of type

$$\frac{d\sigma}{dE d\cos\theta_c} \sim a(E) + b(E)\cos^2\theta_c \quad (2)$$

where  $a(E)$  and  $b(E)$  depend on the ground state wave function and the continuum.

# Experimental technique

## Secondary Beam Production

The secondary beam is produced by fragmentation of a  $^{20}\text{Ne}$  primary beam in a Be target. A primary-beam intensity of  $\sim 1 \times 10^{10}$  ions per spill is required (500 MeV/u, slow-extraction mode). The production cross section of 0.1 mb for  $^{17}\text{Ne}$  isotopes was estimated using the EPAXII formula [33], and the yield on the secondary target was estimated by the Monte-Carlo code MOCADI, including the beam transport through the FRS and the beam-line to Cave C. The expected average  $^{17}\text{Ne}$  beam intensity on the secondary target amounts to about  $1 \times 10^4$  ions/sec.

## Experimental setup

The proposed experiment will be carried out in Cave C using the improved LAND reaction setup. As mentioned earlier, the experimental technique is very similar to that applied in preceding measurements of our collaboration. Two new detector types will be used in addition to detect the proton decay of  $^{17}\text{Ne}$ . These are two large drift chambers placed behind the ALADIN magnet, and Si-strip detectors in front of the magnet where both the  $^{15}\text{O}$  fragments as well as the protons are detected. This will allow a tracking of the protons through the dipole field and thus the determination of their momenta. Protons stemming from quasi-free (p,2p) knockout reactions are detected in a Si-strip barrel surrounding the beam pipe in forward direction (20 to 80 degree) and in the Crystal Ball. The setup is shown schematically in Fig. 5.

The main experimental tasks are the identification and determination of the momenta before and after reaction in the target and detection of all decay products. This is accomplished by means of energy-loss and position measurements with position sensitive pin diodes, a time-of-flight measurement over a large distance between FRS and experimental area, and from the magnetic rigidity determined at the FRS. The heavy fragments emerging after dissociation in the target are again identified and are momentum analyzed using Si-strip detectors placed in between target and the ALADIN Magnet, and using scintillating fibre arrays ( $0.5 \times 0.5 \text{ m}^2$ ) and a two-layer time-of-flight wall ( $0.5 \times 0.5 \text{ m}^2$ ) consisting of 16 position sensitive organic scintillator paddles. Protons from the decay of excited  $^{17}\text{Ne}$  projectiles will be detected with large solid-angle coverage in the forward direction. The gap size of the dipole allows a coverage of about  $\pm 70$  mrad for protons and neutrons, which is sufficient at the beam energy of about 500 MeV/u to cover the excitation energy range of interest (see previous sections). Two position measurements in front (target position, Si-strip detector placed about 1 m behind the target) and two position measurements behind the magnetic field (two drift chambers,  $0.8 \times 1 \text{ m}^2$  active area, 200  $\mu\text{m}$  resolution) allow the determination of the magnetic rigidity and the momenta of protons stemming from the decay of  $^{17}\text{Ne}$ . Finally, time-of-flight and energy-loss information is obtained from a plastic-scintillator wall ( $1.8 \times 1.4 \text{ m}^2$ ) consisting of 32 position-sensitive organic scintillator paddles which also serves for identification. The transverse momenta are obtained from the position measurement in the Si-strip detectors, the longitudinal component from the ToF measurement. In addition, the total momentum is measured by the tracking through the dipole field. A momentum resolution  $\frac{\Delta p}{p} \approx 3 \times 10^{-3}$  is expected. Although neutrons and  $\gamma$ -rays are not very important for the present experiment, they are detected in LAND and in the Crystal Ball detector, respectively. The excitation-energy spectra are obtained from an

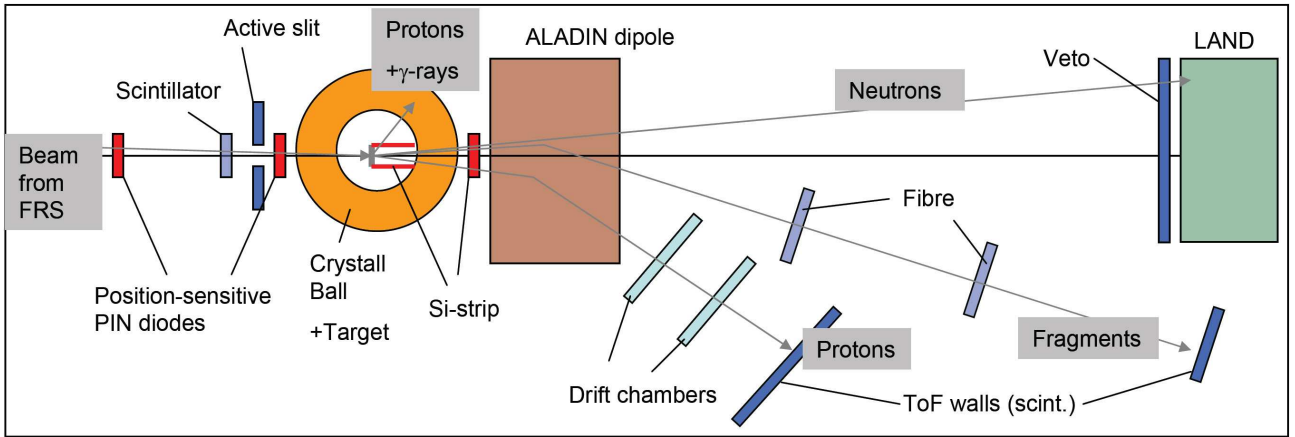


Figure 5: Schematic view of the experimental setup (not to scale). The incoming beam is tracked and identified by means of time-of-flight, energy-loss and position measurements (Scintillator, position-sensitive PIN diodes). The target is surrounded by the Crystal Ball NaI array for detection of photons and protons scattered to large angles. Protons are additionally tracked by Si-strip detectors placed in the forward direction covering an angular range of about 20 to 80 degree. Heavy fragments and projectile-like protons are deflected by the ALADIN dipole field and their momenta are determined by position measurements using Si-strip detectors in front of the magnet and scintillating fibre detectors and drift chambers behind the magnet. Energy-loss and time-of-flight is measured by large-area ToF scintillator walls. Neutrons may be detected by the LAND detector placed at zero degree about 14 m downstream from the target.

invariant-mass analysis. Resolutions amount to about 0.2 MeV at the threshold up to  $\approx 1$  MeV depending on excitation energy. In case of (p,2p) quasi-free knockout reactions induced by the hydrogen ( $\text{CH}_2$ ) target, both protons are detected by Si-strip detectors (20 to 80 degree) and the Crystal Ball. In summary, a kinematical complete measurement of the reaction channels of interest is foreseen.

## Beam request

The proposed experimental programme requires measurements with Pb, C,  $\text{CH}_2$  targets and one without target for background determination. The measurement with Pb target is used to determine the differential cross section for electromagnetic excitation and thus the dipole strength function. A target thickness of  $200 \text{ mg/cm}^2$  is foreseen resulting in a contribution to the invariant-mass resolution similar to the one caused by the detector resolution. Assuming an integrated cross section of about 200 mb, a one-day measurement yields sufficient statistics to extract the dipole strength function, the angle-differential cross section, and to study angular and three-body correlations. The  $\text{CH}_2$  and C targets are used to investigate nuclear reactions. The target thickness is limited in both cases to  $200 \text{ mg/cm}^2$  due to the straggling effects limiting the transverse momentum resolution. A one-day measurement for each target yields sufficient statistics to disentangle the various reaction mechanisms, to extract the differential cross sections, and to identify the different single-particle components in the  $^{17}\text{Ne}$  ground-

state wave function. In addition, one day is required for background measurement, 2 days for debugging the setup, electronic settings, and calibrations. One day is required for FRS settings, calibrations and optimization of the  $^{17}\text{Ne}$  secondary beam.

In total, we request 7 days of beam time. Part of this will be used in parasitic mode prior to the main run for commissioning of the new detectors (drift chambers, Si-strip detectors). We would like to perform the experiment in the second half of the year 2006.

## References

- [1] M.V. Zhukov, I.J. Thompson, Phys. Rev. **C52** (1995) 3505
- [2] A.S. Jensen, K. Riisager, D.V. Federov, E. Garrido, Rev. Mod. Phys. **76** (2004) 215
- [3] B. Jonson, G. Nyman, In *Nuclear Decay Modes*, ed. D.N. Poenaru, IOP Publishing Ltd, Bristol (1996) 102
- [4] M.J.G. Borge *et al.*, Phys. Lett. **B 317** (1993) 25
- [5] A. Ozawa *et al.*, J. Phys. G: Nucl. Part. Phys. **24** (1997) 143
- [6] A.C. Morton *et al.*, Nucl. Phys. **A 706** (2002) 15
- [7] F. Ajzenberg-Selove, Nucl. Phys. **A 460** (1986) 1
- [8] D.J. Millener, Phys. Rev. **C 55** (1997) R1633
- [9] A. Ozawa *et al.*, Phys. Lett. **B334** (1994) 18
- [10] R.E. Warner *et al.*, Nucl. Phys. **A635** (1998) 292
- [11] K. Tanaka *et al.*, Nucl. Phys. **A746** (2004) 532c
- [12] R. Kanungo *et al.*, Phys. Lett. **B 571** (2003) 21
- [13] H. Jeppesen *et al.*, Nucl. Phys. **A739** (2004) 57
- [14] M.J. Chromik *et al.*, Phys. Rev. **C55**(1997) 1676
- [15] M.J. Chromik *et al.*, Phys. Rev. **C66**(2002) 024313
- [16] L.V. Grigorenko, I.G. Mukha, M.V. Zhukov, Nucl. Phys. **A713** (2003) 372; **A740** (2004) 401(E)
- [17] E. Garrido, D.V. Fedorov, A.S. Jensen Phys. Rev. **C68** (2003) 014002
- [18] E. Garrido, D.V. Fedorov, A.S. Jensen Nucl. Phys. **A733** (2004) 85
- [19] L.V. Grigorenko, Yu.L. Parfenova, M.V. Zhukov, Phys. Rev. **C71** (2005) 051604(R)
- [20] K. Hencken, George Bertsch, H. Esbensen Phys. Rev. **C54** (1996) 3043.
- [21] S. K. Charagi, S. K. Gupta, Phys. Rev. **C41** (1990) 1610

- [22] L. Ray, Phys. Rev. **C20** (1979) 1857
- [23] J. Görres, M. Wiescher, F.-K. Thielemann, Phys. Rev. **C51** (1995) 392
- [24] L.V. Grigorenko, M.V. Zhukov, Phys. Rev. **C72** (2005) 015803
- [25] N.B. Shulgina, talk at “*Frontiers in the physics of the Nucleus*” (St. Petersburg, Russia, 2005) Book of Abstracts p.133
- [26] L.V. Chulkov, H. Simon, I.J. Thompson, T. Aumann, M.J.G. Borge, Th.W. Elze, H. Emling, H. Geissel, L.V. Grigorenko, M. Hellström, B. Jonson, J.W.V. Kratz, R. Kulesa, K. Markenroth, M. Meister, G. Münzenberg, F. Nickel, T. Nilsson, G. Nyman, V. Pribora, A. Richter, K. Riisager, C. Scheidenberger, G. Schrieder, O. Tengblad, M.V. Zhukov, Nucl. Phys. **A759** (2005) 23
- [27] L.V. Chulkov, T. Aumann, D. Aleksandrov, L. Axelsson, T. Baumann, M.J.G. Borge, R. Collatz, J. Cub, W. Dostal, B. Eberlein, Th.W. Elze, H. Emling, H. Geissel, V.Z. Goldberg, M. Golovkov, A. Grünschloß, M. Hellström, J. Holeczek, R. Holtzmann, B. Jonson, A.A. Korshennikov, J.V. Kratz, G. Kraus, Y. Leifels, A. Leistenschneider, T. Leth, I. Mukha, G. Münzenberg, F. Nickel, T. Nilsson, G. Nyman, B. Petersen, M. Pfützner, A. Richter, K. Riisager, C. Scheidenberger, G. Schrieder, W. Schwab, H. Simon, M.H. Smedberg, M. Steiner, J. Stroth, A. Suroviec, T. Suzuki and O. Tengblad, Phys. Rev. Lett. **79** (1997) 201
- [28] L.V. Chulkov and G. Schrieder, Z. Phys. **A 359** (1997) 231
- [29] K. Markenroth, M. Meister, B. Eberlein, D. Aleksandrov, T. Aumann, L. Axelsson, T. Baumann, M.J.G. Borge, L.V. Chulkov, W. Dostal, Th.W. Elze, H. Emling, H. Geissel, A. Grunschloss, M. Hellstrom, J. Holeczek, B. Jonson, J.V. Kratz, R. Kulesa, A. Leistenschneider, I. Mukha, G. Munzenberg, F. Nickel, T. Nilsson, G. Nyman, M. Pfützner, V. Pribora, A. Richter, K. Riisager, C. Scheidenberger, G. Schrieder, H. Simon, J. Stroth, O. Tengblad, M.V. Zhukov Nucl. Phys. **A679** (2001) 462.
- [30] H. Simon, D. Aleksandrov, T. Aumann, L. Axelsson, T. Baumann, M.J.G. Borge, L.V. Chukov, R. Collatz, J. Cub, W. Dostal, B. Eberlein, Th.W. Elze, H. Emling, H. Geissel, A. Grünschloss, M. Hellström, J. Holeczek, R. Holtzmann, B. Jonson, J.V. Kratz, G. Kraus, R. Kulesa, Y. Leifels, A. Leistenschneider, T. Leth, I. Mukha, G. Münzenberg, F. Nickel, T. Nilsson, G. Nyman, B. Petersen, M. Pfünzner, A. Richter, K. Riisager, C. Scheidenberger, G. Schrieder, W. Schwab, M.H. Smedberg, J. Stroth, A. Surowiec, O. Tengblad and M.V. Zhukov, Phys. Rev. Lett. **83** (1999) 496
- [31] V. Guimarães, S. Kubono, N. Ikeda, I. Katayama, T. Nomura, M.H. Tanaka, Y. Fuchi, H. Kawashima, S. Kato, H. Toyokawa, C.C. Yun, T. Niizeki, T. Kubo, M. Ohura, M. Hosaka, Phys. Rev. **C 58** (1998) 116
- [32] N. Shulgina, private communication 2005.
- [33] K. Sümmerer and B. Blank, Phys. Rev. C **61** (2000) 034607.